Monolithic integration of quantum well infrared photodetector and modulator

Gilad Almogy,[a] Yuanjian Xu, Andrew Tong, Ali Shakouri, and Amnon Yariv
Department of Applied Physics, California Institute of Technology, Pasadena, California 91125

(Received 13 December 1995; accepted for publication 8 February 1996)

A modulation depth of 40% (0.7 dB/μm) was obtained with an infrared (10.6 μm) modulator consisting of a stack of 50 pairs of weakly coupled asymmetric quantum wells monolithically integrated with a quantum well infrared photodetector. The monolithic integration is shown to be a promising technique for the ''ac'' coupling of infrared focal-plane arrays as well as for the direct study of the effects of electric fields and charge density variations on intersubband transitions.
 [S0003-6951(96)00415-5]

The rapid improvements in the performance of GaAs/AlGaAs quantum well infrared photodetectors[1,2] (QWIPs) utilizing intersubband transitions (ISBTs) along with the well-developed technology of III-V materials has made them natural candidates for fabrication of infrared (IR) focal-plane arrays[3] (FPAs). Several schemes of infrared modulation using the short extinction length and ultrafast response characteristic of ISBTs in quantum wells (QWs) have also been recently demonstrated.[4–6] In this letter we report on the monolithic vertical integration of an optimized quantum well infrared modulator with a QWIP. The results, demonstrated for a single detector element, show the potential for efficient modulation of infrared focal-plane arrays.

Presently, only infrared imaging systems based on pyroelectric detectors are operated in an ''ac'' mode.[7] Modulation is obtained using mechanical choppers with their associated power consumption, size, and reliability limitations. However, with the on going transition from infrared imaging systems based on single detector elements, or lines of detectors, to two-dimensional FPAs there is an emerging need for temporal modulation (chopping) of the infrared scene for photodetectors as well. Integration periods in FPAs are typically limited at 77 K by the dark current saturation of the readout circuits. The introduction of chopping promises to reduce the minimum resolvable temperature difference (MRTD) by increasing the integration period to a full TV rate. Such modulation may be particularly important for QWIPs with their inherently large[8] and spatially nonuniform[9] dark current and may allow background limited operation at temperatures above 77 K.[2]

Electronic modulation of intersubband absorption may be obtained either by a shift of the resonance energy using the ''dc''-Stark effect in asymmetric wells,[4] control of the structure's dipole matrix elements,[5] or by modulation of the quantum well population.[6] The latter was chosen here for its robustness at the high doping densities required and in order to minimize variations in the detector's line shape. External bias was used to move electrons from a narrow well, with a transition energy designed to be at the maximum of the detector's photoresponse, to a wide (reservoir) quantum well with a transition energy only overlapping with the tail of the detector's photoresponse spectrum [Fig. 1(a)]. The structure was designed with a self-consistent numerical solution of the Poisson and Schrödinger equations, taking nonparabolicity and Coloumbic and exchange electron interactions into account.[10]

Neglecting the contribution of carriers in the reservoir well, the absorption in a single pass through the modulator multiquantum well stack is given by[1]

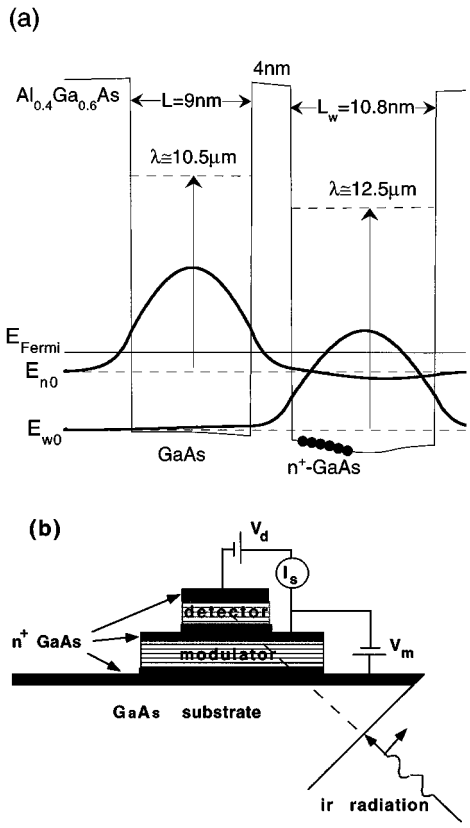

FIG. 1. The band profile of the coupled-quantum well modulator and the ground states in both wells are shown in (a). The energy levels are denoted by the dashed lines and the solid dots denote the intended doping location. A schematic of the integrated device, the biasing circuit, and the light coupling scheme are shown in (b).

[a]Present address: Orbot Instruments Ltd., Industrial Zone P.O. Box 601, Yavne 81106, Israel. Electronic mail:gilad@orbot-instr.co.il

$$A(\Delta E) \equiv -\log_{10}(I_{\text{out}}/I_{\text{in}})$$
$$= \log_{10}(e)\,\frac{2\pi q^2}{n\lambda\epsilon_0}\,\frac{\sigma\mu^2}{\Gamma[1+(\Delta E/\Gamma)^2]}\,\frac{\sin^2(\theta)}{\cos(\theta)}, \quad (1)$$

where λ is the optical wavelength, n the refractive index, θ the angle between the polarization vector and the plane of the quantum wells, q the electron charge, and ϵ_0 the vacuum permittivity. The dipole matrix element, the transition's half-width at half-maximum (HWHM) energy, the total surface charge density in the narrow wells, and the detuning energy are defined as : μ, Γ, σ, and ΔE, respectively. Assuming that the Fermi level is above both ground subbands, that there is no thermal distribution of charges, and that the wave functions remain unmodified by the electric field, we can solve for the charge transfer as a function of applied bias. Taking screening into account but maintaining fixed voltage boundary conditions,[11] the surface charge transfer with applied bias *(V)* is simply derived as

$$\sigma(V) = \frac{\epsilon V/q}{(1+1/y)L_p - L_w}, \quad (2)$$

where ϵ is the static dielectric constant ($\epsilon_{\text{GaAs}} \cong 13.1$), L_p the structure period, $L_w \equiv |\langle\psi_{n0}|z|\psi^*_{n0}\rangle - \langle\psi_{w0}|z|\psi^*_{w0}\rangle|$ is the separation between the ground states of the narrow and wide quantum wells: Ψ_{n0} and Ψ_{w0}, respectively. We have defined the screening factor as $y \equiv m^* q^2 L_w/2\pi^2\epsilon$, where m^* is the effective mass.

The integrated device, designed for 10.6 μm operation and for maximizing the modulator's dynamic range, was grown by molecular beam epitaxy (MBE). A 0.6 μm n^+-GaAs contact layer and a 0.2 μm GaA buffer layer are grown on a semi-insulating GaAs substrate. The growth sequence of each of the 50 modulator periods [Fig. 1(a)] consisted of a 9 nm undoped GaAs well, a 3 nm undoped $Al_{0.4}Ga_{0.6}As$ separation barrier, and a 10.8 nm storage well. The latter was Si doped to a nominal volume density of 2×10^{18} cm^{-3} in a 4 nm thick region beginning 0.5 nm away from the barrier. From the total absorption of both narrow and wide wells we deduce that the actual doping density is approximately 20% higher than the intended value. The periods were separated by 42.2 nm $Al_{0.4}Ga_{0.6}As$ barriers. The QWIP was grown on top of the modulator after another 0.2 μm GaAs buffer layer and a 0.6 μm n^+-GaAs contact layer. It consisted of 15 6.5 nm thick Si-doped GaAs QWs with a nominal doping density of 1.1×10^{12} cm^{-2} and 16 44 nm thick $Al_{0.18}Ga_{0.82}As$ barriers. Single element mesas where fabricated in a two-step etching process and an edge of the sample was polished to 45° to couple IR radiation in accordance with the intersubband selection rules[2] [Fig. 1(b)].

The detector's photoresponse at an operating temperature of 10 K and under a constant bias of 0.8 V is plotted in Fig. 2 for modulator biases of −13 V (36 kV/cm) and +14 V (38 kV/cm). The maximal modulation depth obtained, roughly 40%, corresponds to a modulation of 0.7 dB/μm in the 3.15 μm thick modulator. The modulator's absorption is measured from the change in the detector's photospectrum as a function of modulator bias and fitted with a Lorentzian line shape [Eq. (1)]. From the fit parameters we deduce the bias dependence of the intersubband transitions shown in Fig. 3.

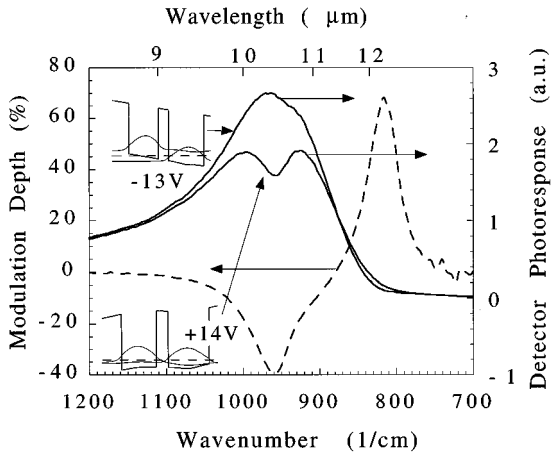

FIG. 2. The detector's photoresponse for a negative (−13 V) and positive (+14 V) modulator bias leading to the depletion and the filling of the narrow well, respectively (solid curves). Their ratio gives the modulation depth (dashed curves). The corresponding modulator's band structure is shown in the insets with the solid curves showing the calculated ground states and the dashed lines denoting the Fermi levels.

Using the calculated dipole matrix elements the surface density in the narrow well is calculated [Fig. 3(a)]. It displays a linear increase with applied bias up to a value of roughly 5×10^{11} cm^{-2}, with a slope that agrees with the numerical self-consistent model but is roughly 15% greater than expected from Eq. (2). This is attributed to the exchange interaction which is included only in the numerical model and reduces the Coloumbic repulsion.[10] At zero bias the charge in the narrow well is seen to be only 5% of the total popu-

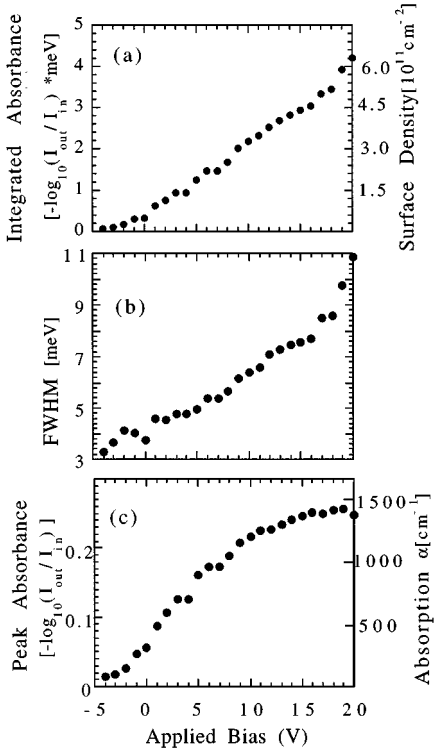

FIG. 3. The integrated absorption (a), the transition energy broadening (b), and the peak absorption (c) of the modulator's narrow well as a function of applied bias.

lation. This inconsistency with the designed value of 20% is attributed to donor segregation[12] of roughly 3 nm along the growth direction, i.e., away from the narrow well. It has little effect on the absorption wavelength but limits the modulator's dynamic range as several volts of negative bias completely deplete the well. The modulators peak absorption at 10.5 μm is about one meV away from the designed value as well as from the detector's photoresponse maximum (Fig. 2).

The increased broadening with increased surface density displayed in Fig. 3(b) causes a saturation of the maximal absorption [Fig. 3(c)] at a surface density of roughly 5×10^{11} cm^{-2}. Although some further improvement may be possible through a larger separation of the carriers and doping and improved material quality, the maximal peak absorption per period is inherently limited by the increasing broadening. More periods of the coupled quantum well structure or increased optical confinement will therefore be required to approach full extinction. Finally, it should be noted that the maximal operating temperature of intersubband modulators is not a direct function of the operating wavelength as is that of QWIPs.[8] Since the operating temperature is only limited by the quantum well band offsets and material quality, intersubband modulators may potentially be hybridized to infrared detectors operating at higher temperatures.

G. Almogy would like to acknowledge many fruitful discussions with I. Bar-Joseph and U. Meirav of the Weizmann Institute. This work was funded in part by AFOSR, ARPA, and the Office of Naval Research under Award No. N00014-91-J-1195.

[1] L. C. Chiu, J. S. Smith, S. Margalit, A. Yariv, and A. Y. Cho, Infrared Phys. **23**, 93 (1983).
[2] B. F. Levine, J. Appl. Phys. **74**, R1 (1993).
[3] T. S. Fasaka, W. A. Beck, J. W. Little, A. C. Goldberg, B. Rosner, and M. Stegall, Proceedings of SPIE Infrared Imaging Systems: Design, Analysis, Modeling and Testing IV vol. 1969-25 (1993); L. L. J. Kozlowski, G. M. Williams, G. J. Sullivan, C. W. Farley, R. J. Anderson, J. Chen, D. T. Cheung, W. E. Tennant, and R. E. DeWames, IEEE Trans. Electron. Devices **38**, 1124 (1991); C. G. Bethea, B. F. Levine *et al. ibid.* **40**, 1957 (1993).
[4] E. Martinet, F. Luc, E. Rosencher, Ph. Bois, and S. Delaitre, Appl. Phys. Lett. **60**, 895 (1992).
[5] J. Faist, F. Capasso, A. L. Hutchinson, L. Pfeiffer, and K. C. West, Phys. Rev. Lett. **71**, 3573 (1993).
[6] N. Vodjdani, B. Vinter, V. Berger, E. Bockenhoff, and E. Costard, Appl. Phys. Lett. **59**, 555 (1991).
[7] C. M. Hanson, SPIE Infrared Technol. **XIX**, 2020, 330 (1993).
[8] M. A. Kinch and A. Yariv, Appl. Phys. Lett. **55**, 2093 (1989).
[9] V. Swaminathan, in NATO Advanced Research Workshop on Quantum Well Intersubband Transition Physics and Devices, September 1993, Whistler, Canada (only appearing in abstracts—not in proceedings).
[10] G. Almogy, Ph.D., thesis, California Institute of Technology, 1995.
[11] Standard self-consistent solutions which use electric field boundary conditions, e.g., W. Q. Chen and T. G. Andersson, J. Appl. Phys. **73**, 4484 (1993), overestimate the effects of screening. The electric field must be found iteratively to match the applied voltage.
[12] H. C. Liu, Z. R. Wasilewski, M. Buchanan, and H. Chu, Appl. Phys. Lett. **63**, 761 (1993).